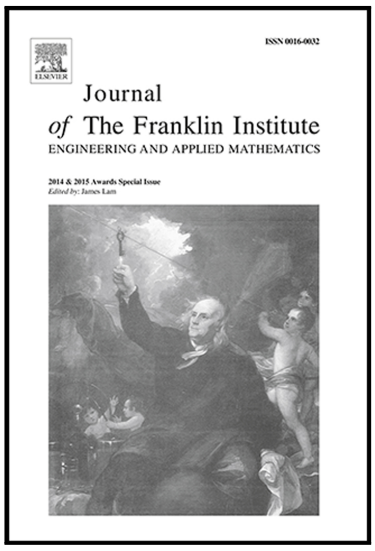

Optimal Non-Parametric Tuning of PID Controllers Based on Classification of Shapes of Oscillations in Modified Relay Feedback Test

Ahmed Rehan , Igor Boiko , Yahya Zweiri

PII: S0016-0032(20)30803-6
DOI: https://doi.org/10.1016/j.jfranklin.2020.12.007
Reference: FI 4890

To appear in: *Journal of the Franklin Institute*

Received date: 29 June 2020
Revised date: 20 October 2020
Accepted date: 8 December 2020

Please cite this article as: Ahmed Rehan , Igor Boiko , Yahya Zweiri , Optimal Non-Parametric Tuning of PID Controllers Based on Classification of Shapes of Oscillations in Modified Relay Feedback Test, *Journal of the Franklin Institute* (2020), doi: https://doi.org/10.1016/j.jfranklin.2020.12.007

Optimal Non-Parametric Tuning of PID Controllers Based on Classification of Shapes of Oscillations in Modified Relay Feedback Test

Ahmed Rehan [a,b], *Igor Boiko* [a,b], *Yahya Zweiri* [b,c]
[a]Electrical Engineering and Computer Science Department, Khalifa University, Abu Dhabi, UAE
[b]Khalifa University Center for Autonomous Robotic Systems (KUCARS), Khalifa University, Abu Dhabi, UAE
[c]Aerospace Engineering Department, Khalifa University, Abu Dhabi, UAE.

ABSTRACT

In this work, tuning rules of the PID controller have been developed by categorizing a system's response into distinct classes. The classes are formed using the shapes of the test oscillations induced by the system under the Modified Relay Feedback Test (MRFT) produced by specific system models. It is proposed that a physical system can be categorized into one of the proposed classes and thus the tuning rules for a particular class can apply to any kind of system from this class. The idea of producing tuning rules that are based on the shape of the oscillations induced in the loop containing the process comes from the observations that oscillatory responses of physical systems reveal just a few different shapes depending on system dynamics. For applying the developed optimal tuning rules for an arbitrary system, first, certain system characteristics are determined using *a priori* knowledge of the class model. Then the system's response with the application of the MRFT is examined to classify the oscillation waveform/shape. In this work, such classification is carried out using a cross-correlation algorithm. Finally, a class tuning rules are applied.

Index Terms— *PID Controller, PID Tuning, Modified Relay Feedback Test, Relay Feedback Test, Shape-based Tuning, Response Classification*

1. INTRODUCTION

PID is one of the control techniques that is widely applied in the industry and is still researched by the academic community. The major challenge of PID control design is tuning of its parameters, as every system requires a different combination of PID parameters for its optimum performance. The tuning of PIDs is usually categorized into two methods: parametric tuning and non-parametric tuning. The former involves identification of a process model. The latter, on the other hand, do not require model identification and involve some measurable characteristics of a process. These characteristics are only evident in certain of tests that reveal dynamics of the process. Most of the research efforts in PID tuning have been applied to parametric tuning methods. For non-parametric methods, very few works were reported. The earliest prominent works, in this regard, were by Ziegler and Nichols (Z-N) who pioneered the area of non-parametric tuning by proposing two methods based on time and frequency domain measurements [1]. The time-domain test relied on the idea that many systems in the process industry exhibit a step response as an 'S' shaped curve. This characteristic shape can be used to extract certain parameters that can aid in the tuning process. This idea was modified by Cohen & Coon [2], who proposed to use the same 'S' shaped curve to position dominant poles of a system to improve load

disturbance rejection. The Z-N frequency domain test used proportional gain in closed-loop to induce oscillations of a process at its ultimate frequency [1]. The tuning rules in this case were a function of ultimate frequency and ultimate gain of the test oscillations. Later, Astrom and Hagglund (A-H) proposed another frequency-domain test, the Reay Feedback Test (RFT) [3]. In this test, a simple on-off relay can be used in closed-loop to induce oscillations in a process that can provide an estimate of the ultimate frequency and gain of a system [4]. A-H test originated a new field of control tuning, known as auto-tuning. Later on, the basic concept of the A-H RFT test was extended in many forms; relay with a delay [5]-[6], a two-channel relay with integrator [7], a two-channel relay with differentiator [8], saturation relay [9], etc. Other recent trends in the PID tuning can be referred in [31].

The Modified Relay Feedback Test (MRFT)[10] is an advancement of RFT, in which the oscillations can be excited in the third or second quadrants of the Nyquist plot. This is done through using a relay having switching points that vary as a linear function of the last-occurring extremum of error signal [3]. The MRFT takes into account the fact that introducing a controller changes the gain and phase margins of a closed-loop system thereby changing its phase cross-over frequency. Such a change in frequency behavior can be controlled by using an MRFT parameter through which the degree of lag or advance in the relay switching is adjusted. Moreover, the homogenous formulation of the tuning rules coupled with the MRFT makes it applicable to a wide range of processes having proportionally related time constants and gains. Various implementations of the MRFT have proven its capability to fine-tune PIDs for a variety of mechatronic and process systems [11]–[15].

Most of auto-tuning methods of PID controllers are parametric; they rely on certain process models, which are treated as representing true dynamics of a particular process, despite many of them are approximations and do not reflect the physical principles. This approach to the controller design constitutes the so-called *certainty equivalence principle*. However, in practical situations, no physical system can be characterized by an exact model. There is always a mismatch between the dynamic model describing a process and the actual dynamics of this process. Non-parametric tuning methods can potentially be free from the noted drawback, but only if tuning rules are designed in a special way. The solution to this problem was proposed in [16], [17] with the introduction of process-specific optimal non-parametric tuning rules and treating the formulated problem as *optimization under uncertainty*. To the best knowledge of the authors, [17] and the book [16] provide the only method that provides a framework for designing tuning rules applicable to a range of models. Models are still used, with parameters treated as *situational*, but only for a description of a class of systems and at the stage of tuning rules design. In its application, the method is totally model-free. The tuning rules are also coupled with the MRFT, can serve as a very effective tool for non-parametric tuning of systems.

In the present work, we aim to design optimal tuning rules and couple them with the MRFT and to enhance tuning though using shapes of the system's self-oscillatory response. The idea of using shapes of the response of a process is known but very few works have been reported in this regard. Most of the works are focused on using the shapes for identification purposes and the shapes are generated by exciting a process in RFT oscillatory mode. It started from Luyben's work [18], who investigated three unique shapes of First Order Plus Deadtime (FOPDT) models excited under RFT mode. The idea was to use the different dead time to time constant (D/τ) ratios to generate different shapes of RFT waveform. To characterize the shapes, he proposed a quantifying factor specifically to quantify the curvature in RFT shapes. For each class, the most optimal tuning rules were derived using Z-N, Tyreus Luyben (T-L), and Internal Model Control (IMC) methods. Thyagarajan extended the same idea to categorize RFT shapes of first, second, and higher-order systems [19]. Based on a resemblance between the shape of the RFT response and a class response, the process class was determined which was further verified using

frequency domain Integral Absolute Error (IAE). Optimal tuning rules of PI control based on T-L, Z-N, minimum ITAE, and IMC were proposed for each identified model. Later, Thyagarajan also proposed to use RFT with controller in loop to assess the controller's performance [20]. Four classes of RFT responses were considered for FOPDT and PI controller. It was argued that the best performance of FOPDT with PI controller is obtainable at a specific ϵ/D, ϵ being ratio of integral time constant and closed loop gain. Based on the shapes, compensation factors can be computed that can adjust the controller to get the best optimal performance. Similarly, Panda [21] used second and first-order models to form three classes using RFT limit cycles. His work was based on using analytical expressions of each model and RFT data points to do the identification. Optimum control settings of TL, IMC-Chien, and IMC-Mac were developed for each model class.

Esakkiappan [22] used RFT shapes to approximate the model of the Inverse Response plus Time Delay (IRPTD) process. A general analytical expression to characterize the output response of the IRPTD process was derived. The expression was used to identify the parameters of the system using boundary conditions and experimental data of RFT waveforms. Thyagarajan [23] worked on a similar idea and used the identified model to design an IMC based PID controller for the process. Tao used exact relations of output responses of Second-Order Plus Dead Time (SOPDT) models for model identification [24]. Three forms of models were investigated in his work: overdamped, critically damped, underdamped, and three corresponding algorithms were proposed to fit the models with RFT responses of example processes. Also, guidelines to design the Butterworth filter and statistical averaging method were proposed to cope with noisy waveforms. IMC control was developed from identified models and was tested on higher order systems to prove the identification accuracy.

Various techniques were also focused on improving the approximation that comes from treating the shape of the RFT waveform as a sine wave instead of a square wave. Some methods, for example [25], have used high order terms of the Fourier series of a square wave. A significant improvement in ultimate parameter estimation was reported using saturation relay [9] whose output is proportional to input along with a multiplicative gain, which saturates at a certain value. With this scheme, the output resembles a truncated sinusoid. The saturation gain is bounded between two extremes that generate pure sinusoid or no oscillations. A test was proposed to find minimum gain and an optimal gain procedure was formulated that gives the best approximation of the ultimate parameters of the RFT test. Various other schemes also exist that approximate model using RFT data. A good account of some of the approaches can be found in [9].

From all the reported works, it is observed that in relay-oscillatory mode, the shape of the system's response varies with its parameters. However, for the entire domain of model parameters, only a few different shapes are exhibited by a system's model. These distinct shapes correspond to specific subsets of the process model. These subsets can be singled out through partitioning of the space of model parameters, which are called in this task *situational parameters* [16], [17]. In the present work, it is proposed that such partitions can be determined from the shapes of the test oscillations (induced by the MRFT). These partitions are used to form classes where an optimal tuning rule can be designed for each class. The classes are unique with respect to a shape and a type of the process model. For tuning rules, the optimum non-parametric tuning method of [16], [17] combined with the MRFT [10] is used to derive tuning rules for the range of models. We categorize the models of LTI systems into a few classes. Five kinds of system models are investigated in this respect. These models, in the self-oscillatory mode, exhibit four kinds of oscillation shapes. It is proposed that the tuning rules for these classes can be applied to any physical system by determining the class of the system using a classification algorithm. A cross-correlation based classification is also proposed for such a purpose.

2. MOTIVATION OF SHAPE BASED TUNING RULES

Exciting systems to produce limit cycles is one of the most practiced ways to perform PID tuning. The oscillatory response of the relay feedback system possesses unique properties and can provide very important information for the tuning of PID controllers. Based on the conventional tuning methods, a satisfactory tuning can be carried out by just using the information of the ultimate frequency and ultimate gain of a system. For example, the tuning rules of Z-N are just a basic function of the frequency of the oscillations and the gain at which the marginal stability is achieved. The A-H test is also based on a similar idea where frequency and amplitude of the oscillations in RFT are used to approximate the ultimate parameters. Other extensions of the relay feedback test somehow are aimed at improvement of the approximation using different experimental configurations or using modified mathematical methods. Essentially, the approximation works best only for the processes with low pass characteristics. The RFT response of such systems resembles sinusoid waveform and hence describing function analysis is used to compute ultimate parameters and then the PID gains. However, the performance of these rules deteriorates as the process loses its low-pass characteristic and the RFT response shape becomes non-sinusoidal. This is a drawback of tuning that is based on the relay feedback test and the tuning rules that account only for the first harmonic approximation of the signals. The practice of tuning shows that different systems may exhibit different oscillatory shapes in the RFT/MRFT, but exhibit the same frequency and amplitude. In this respect, the use of shape for differentiating between these distinct classes of systems would provide an opportunity for increasing the accuracy of tuning.

We propose using the shape of the system's response to further extend the concept of tuning methods based on the frequency and ultimate gain. In self-oscillatory mode under the RFT/MRFT, each system exhibits a unique response profile identified by a certain geometric shape. Since such an appearance of the system's response is peculiar to its mathematical model, we can have an indefinite number of shapes for innumerable structures of models. However, we aim to represent all the systems using five models with the proposition that these models can accurately represent many kinds of physical systems for the purpose of controller tuning. This is due to the fact that the majority of the system's behavior can be described by a few *implied process models*[1] (to be presented in the next section). The self-oscillatory response of these implied models exhibits four kinds of distinct shapes: Sinusoid, Wavy, Curved Triangular, and Triangular (Figure 3). Hence, we organize all the classes using five models and four oscillations shapes. It is proposed that any physical system can be categorized into these classes; hence the tuning rules formulated for these classes can be applied to many kinds of systems found in real-world applications.

3. MATHEMATICAL MODELING OF PERIODIC MOTION IN RELAY FEEDBACK SYSTEMS

To investigate what the waveform shape looks like, we need to model the periodic motion of a relay feedback system. The modeling is essentially a mathematical characterization of a single cycle of periodic motion. Since the shape of the response is irrespective of the relay hysteresis value, it is observed that the shapes do not change whether we operate the system in RFT or MRFT mode. Hence we use generalized modeling in this respect which would apply to both kinds of tests.

[1] The notion of implied process model was introduced in [16], [17] to describe a process model that can be used for optimal tuning rules design.

The selection of systems is critical in the categorization of system models and the oscillation shapes. The models are chosen to generalize the maximum number of physical systems. In this respect, the best categorization of systems can be done using five LTI models having the following transfer functions:

$$G_1 = \frac{e^{-\tau s}}{s} \tag{1}$$

$$G_2 = \frac{e^{-\tau s}}{s+1} \tag{2}$$

$$G_3 = \frac{e^{-\tau s}}{s^2 + 2\zeta s + 1} \tag{3}$$

$$G_4 = \frac{e^{-\tau s}}{s(s+1)} \tag{4}$$

$$G_5 = \frac{e^{-\tau s}}{s(s^2 + 2\zeta s + 1)} \tag{5}$$

Where 'τ' is a deadtime and 'ζ' is a damping ratio. The transfer functions (1)-(5) have unity time constants and gain and it is intended to derive homogenous tuning rules (see [16], [17]) based on these models that would be applicable generally irrespective of time constant and gain of the system. The transformation of any 1st to 3rd order model into the above forms can be done by normalization procedure, where the model is divided by its gain 'k' and the time constant is absorbed into Laplace variable as $s' = Ts$. With this method, we are able to produce more generalized and homogenous tuning rules for a wide category of systems, having similar form but different gains and time constants.

The time response of models (1)-(5) have been derived in some of the works [19], [21], [24]. The methodology of these works is tedious and lengthy as it applies to individual cases and changes significantly from one system to another. In this work, it is intended to use a universal framework to mathematically model the time responses for general LTI systems and use the model equations to simulate the oscillation shapes.

3.1. MODEL OF OSCILLATIONS IN RELAY SYSTEMS

In a relay feedback system, self-excited periodic motions (limit cycle) exist subject to fulfillment of the following three conditions [3]: (i) the existence of a periodic solution of the system equations, which can be established, for example, by the Locus of a Perturbed Relay System (LPRS) method [3]: (ii) orbital stability of the established periodic solution (these conditions were provided by Asrom [3], [4], and for the systems containing delays in [27]); (iii) initial condition must be selected in such a way (usually close enough to the limit cycle) that would provide the transition to the limit cycle (periodic motion). There can be some systems having both a limit cycle and a stable equilibrium point and hence, for a certain set of initial conditions, the system trajectories may converge to the equilibrium point instead of the limit cycle [30].

In this paper, we consider the models (1)-(5) that represent stable systems for which all the above three conditions are satisfied. For the derivation of periodic solution, consider a general system representation in the following form where the system is supposed to be connected with an ordinary relay:

$$\dot{x}(t) = Ax(t) + Bu(t-\tau)$$
$$y(t) = Cx(t) \tag{6}$$

where $A \in R^{n\,x\,n}$, $B \in R^{n\,x\,1}$, $C \in R^{1\,x\,n}$. In the relay feedback setting, the response of the models (1)-(5) is fundamentally a solution of the state equations operating back and forth around equilibrium between two inputs, $u(t) = \pm 1$. Such an input of relay is formulated as follows:

$$u(t) = \begin{cases} 1 & \text{if } e(t) \geq \mathrm{b} \\ -1 & \text{if } e(t) < -\mathrm{b} \end{cases} \tag{7}$$

where '$2b$' is the hysteresis value. The solution of (6) under the input (7) is periodic and constitutes a positive half cycle $y^+(t)$, and a negative half cycle $y^-(t)$.

We aim to derive a mathematical formula of the periodic motion (oscillation waveform) of unity amplitude in a relay feedback system. First, consider the case of the models without any integrator. Note that *'A'* is invertible for such cases. The output response based on the LTI systems theory is given as:

$$\tilde{x}(t) = e^{A(t-\tau)}\tilde{x}(\tau) \pm A^{-1}(e^{A(t-\tau)} - I)B$$

For the positive cycle,

$$x^+(t) = e^{\mathrm{A}(t-\tau)}\tilde{\mathrm{x}}(\tau) - \mathrm{A}^{-1}(e^{A(t-\tau)} - \mathrm{I})\mathrm{B}$$

where $\tilde{\mathrm{x}}(\tau)$ and $\tilde{\mathrm{x}}(0)$ are given according to [16] as:

$$\tilde{\mathrm{x}}(\tau) = e^{\mathrm{A}\tau}\tilde{\mathrm{x}}(0) - \mathrm{A}^{-1}(e^{\mathrm{A}\tau} - \mathrm{I})\mathrm{B}$$
$$\tilde{x}(0) = (I + e^{\frac{A\pi}{\omega}})^{-1}(I + e^{A\pi/\omega} - 2e^{A(\frac{\pi}{\omega}-\tau)})A^{-1}B$$

Merging all above 3 equations gives the following solution for the positive half-cycle:

$$x^+(t) = e^{\mathrm{A}t}\left(\mathrm{I} + e^{\frac{\mathrm{A}\pi}{\omega}}\right)^{-1}\left(\mathrm{I} + e^{\frac{\mathrm{A}\pi}{\omega}} - 2e^{\mathrm{A}\left(\frac{\pi}{\omega}-\tau\right)}\right)\mathrm{A}^{-1}\mathrm{B} - e^{\mathrm{A}(t-\tau)}\mathrm{A}^{-1}(e^{\mathrm{A}\tau} - \mathrm{I})\mathrm{B} - \mathrm{A}^{-1}(e^{\mathrm{A}(t-\tau)} - \mathrm{I})\mathrm{B}$$

The output of the positive half-cycle is mathematically given in the following form:

$$y^+(t) = C\left(e^{\mathrm{A}t}\left(\mathrm{I} + e^{\frac{\mathrm{A}\pi}{\omega}}\right)^{-1}\left(\mathrm{I} + e^{\frac{\mathrm{A}\pi}{\omega}} - 2e^{\mathrm{A}\left(\frac{\pi}{\omega}-\tau\right)}\right)\mathrm{A}^{-1}\mathrm{B} - e^{\mathrm{A}(t-\tau)}\mathrm{A}^{-1}(e^{\mathrm{A}\tau} - \mathrm{I})\mathrm{B} - \mathrm{A}^{-1}\left(e^{\mathrm{A}(t-\tau)} - \mathrm{I}\right)\mathrm{B}\right) \tag{8}$$

In the same way, the output of the negative cycle can be derived.

$$y^-(t) = C\left(e^{\mathrm{A}(t-\tau)}\left[\left(\mathrm{I} - e^{\mathrm{A}\frac{2\pi}{\omega}}\right)^{-1}\mathrm{A}^{-1}\left[2e^{\mathrm{A}\theta} - e^{\mathrm{A}\frac{2\pi}{\omega}} - \mathrm{I}\right]\mathrm{B} - \mathrm{A}^{-1}(e^{\mathrm{A}\tau} - \mathrm{I})\mathrm{B}\right] + e^{\mathrm{A}(t-\tau)}\mathrm{A}^{-1}(e^{\mathrm{A}\tau} - \mathrm{I})\mathrm{B} + \mathrm{A}^{-1}\left(e^{\mathrm{A}(t-\tau)} - \mathrm{I}\right)\mathrm{B}\right) \tag{9}$$

The frequency 'ω' represents the frequency of the oscillations in the system under the RFT/MRFT mode. It is assumed that this frequency is directly measurable from the output response. In analysis, we compute it using mathematical tools of the Describing function, the Locus of Perturbed Relay Systems

(LPRS), the Tsypkin locus, and the Hamel method [26]–[28]. In this work, we use the LPRS method for the determination of ω [16], which is more convenient than the former due to the possibility of using the matrix description. Based on this method, we need to solve the following equation for each model (1)-(5):

$$Im\,J(\Omega) = -\frac{\pi b}{4h} \tag{10}$$

where $J(\omega)$ is the LPRS, 'Ω' is the frequency of the periodic solution (see [16]). In comparison, ω is an arbitrary frequency of the LPRS.

For the computation of oscillation frequency $\omega = \Omega$, the equation (10) must be solved for Ω, with the LPRS function given by [16]:

$$J(\omega) = -\frac{1}{2}C\left[A^{-1} + \frac{2\pi}{\omega}\left(I - e^{\frac{2\pi}{\omega}A}\right)^{-1} e^{\left(\frac{\pi}{\omega}-\tau\right)A}\right]B + j\frac{\pi}{4}C(I + e^{A\pi/\omega})^{-1}(I + e^{A\pi/\omega} - 2e^{A(\pi/\omega-\tau)})A^{-1}B \tag{11}$$

It should be noted that the real part of $J(\omega)$ contains information about the equivalent gain of the relay [3], and the imaginary part comprises the condition of the switching of the relay and, consequently, contains information about the frequency of the oscillations.

The above equations (8)-(11) are only applicable to the models without any integrator part (i.e. $1/s$). For integrating processes, the matrix A if the model (6) is non-invertible, hence we need a different approach to derive the periodic solutions. Consider an integrating system defined by the following:

$$\begin{aligned} \dot{x}(t) &= Ax(t) + Bu(t-\tau) \\ \dot{y}\,(t) &= Cx(t) \end{aligned} \tag{12}$$

Note above that the matrix A is invertible despite the fact that the process is integrated, because the integrator acts separately on an intermediate output '$y^* = Cx$' to produce the actual output, i.e. $y = \int_0^t Cx(t)dt$.

The positive and the negative half-cycles for this case are written as:

$$y^+(t) = y(0) - CA^{-1}Bt + CA^{-1}[(e^{At} - I)\rho + A^{-1}(e^{At} - I)B] \tag{13}$$

$$y^-(t) = y(\theta_1) + CA^{-1}Bt + CA^{-1}[(e^{At} - I)\eta - A^{-1}(e^{At} - I)B] \tag{14}$$

The variables ρ, η, $y(0)$ and $y(\theta_1)$ are given as follows:

$$\rho = \left(I - e^{\frac{2A\pi}{\omega}}\right)^{-1} A^{-1}\left[e^{\frac{2A\pi}{\omega}} - 2e^{\frac{A\pi}{\omega}} + I\right]B$$

$$\eta = \left(I - e^{\frac{2A\pi}{\omega}}\right)^{-1} A^{-1}\left[3e^{\frac{A\pi}{\omega}} - I\right]B$$

$$y(0) = CA^{-1}B\frac{1}{2}\frac{A\pi}{\omega} + \frac{1}{4}CA^{-2}\left\{\left(I - e^{\frac{2A\pi}{\omega}}\right)^{-1}\left[6e^{\frac{2A\pi}{\omega}} - 6e^{\frac{A\pi}{\omega}} - 2e^{\frac{3A\pi}{\omega}} + 2I\right] - 2e^{\frac{A\pi}{\omega}} + 2I\right\}B$$

$y(\theta_1) = -y(0)$,

where the oscillation frequency $\omega = \Omega$ is calculable from the following LPRS function:

$$Im\,J(\Omega) = -\frac{\pi b}{4h} \tag{15}$$

For the computation of oscillation frequency, we equate the above equation to the imaginary part of the following [29]:

$$\begin{aligned} J(\omega) = \frac{1}{4}\,CA^{-2}\left\{(I-D^2)^{-1}\left[D^2-\left(I+\frac{4\pi}{\omega}\,A\right)D+D^3-I\right]+D-I\right\}B \\ +j\frac{\pi}{8}\,CA^{-1}\left\{\frac{\pi}{\omega}\right. \\ \left.+A^{-1}[(I-D^2)^{-1}\,(3D^2-3D-D^3+I)-D-I]\right\}B) \end{aligned} \tag{16}$$

where $D = e^{\frac{\pi}{\omega}A}$. Equations (8)-(11), and (13)-(16), form the basis of the modeling equations for all the LTI systems undergoing periodic motion in relay feedback mode. To apply these equations, we need to transform the transfer functions (1) – (5) into the state-space models given by (6) or (12), depending on whether the process is self-regulating (non-integrating) or integrating. The waveforms can be determined through the formulas (8), (9), (13) and (14).

3.2. THE MODIFIED RELAY FEEDBACK TEST (MRFT)

To investigate and characterize the shapes of the responses, we analyze the system by operating it in the MRFT setting. The use of the MRFT instead of the conventional relay is beneficial as allows one to produce oscillations in 2nd and 3rd quadrants of the Nyquist plot of the process [10], which better serves the PID controller design. Moreover, tuning rules that provide the desired gain or phase margins can be derived [10]. Figure 1 shows the schematic implementation of the MRFT. The system is connected in feedback with the MRFT block and oscillations are excited with infinitesimally small initial condition i.e. $x(0) = \lim_{\delta\to 0}\delta$ (Figure 1). The purpose of such initial condition is to initiate the first switching of the relay. The initial condition dies down with time, but the oscillation continues.

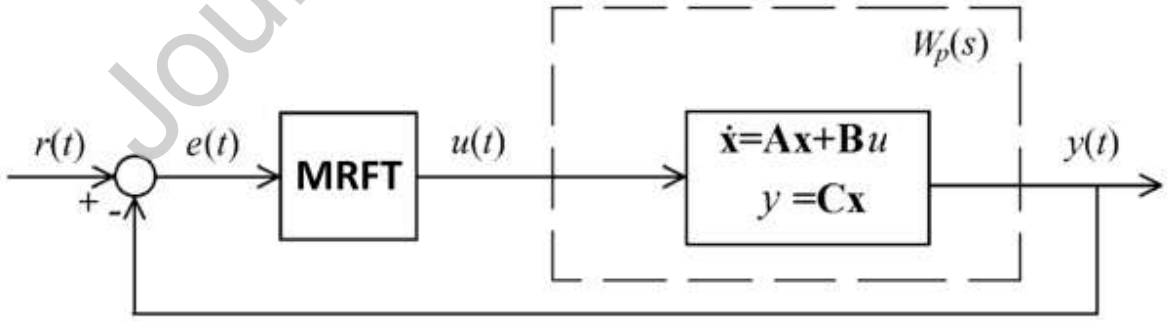

Figure 1 Schematic setting of the MRFT implementation

Essentially, the idea of the MRFT is to control the switching points of a relay as a linear function of the latest extremum of error. By such controlled switching of the relay, one can easily apply the theory of MRFT to achieve the desired phase or gain margin of the closed-loop system. Mathematically the relay output $u(t)$ is formulated as follows.

$$u(t) = \begin{cases} h & \text{if } e(t) \geq b_1 \text{ or } (e(t) > -b_2 \text{ and } u(t-) = h) \\ -h & \text{if } e(t) \leq -b_2 \text{ or } (e(t) < b_1 \text{ and } u(t-) = -h) \end{cases}$$

where, $b_1 = -\beta e_{min}, b_2 = \beta e_{max}$ The extreme values $e_{max} > 0$ and $e_{min} < 0$ correspond to the last maximum and minimum values of e(t) after crossing the zero level; $u(t-) = lim_{\epsilon \to 0} u(t - \epsilon)$ is the control
value at the time immediately preceding the current time '*t*'; *'h'* is the amplitude of the relay; 'β' is a constant that determines the switching point of the oscillation. Figure 2 shows a typical waveform of a system excited in MRFT mode. Once sustained oscillations are established, the frequency and gain of the oscillations are recorded and further used in the tuning process. Section 5 details the process of developing tuning rules using the information of frequency and ultimate gain of the process.

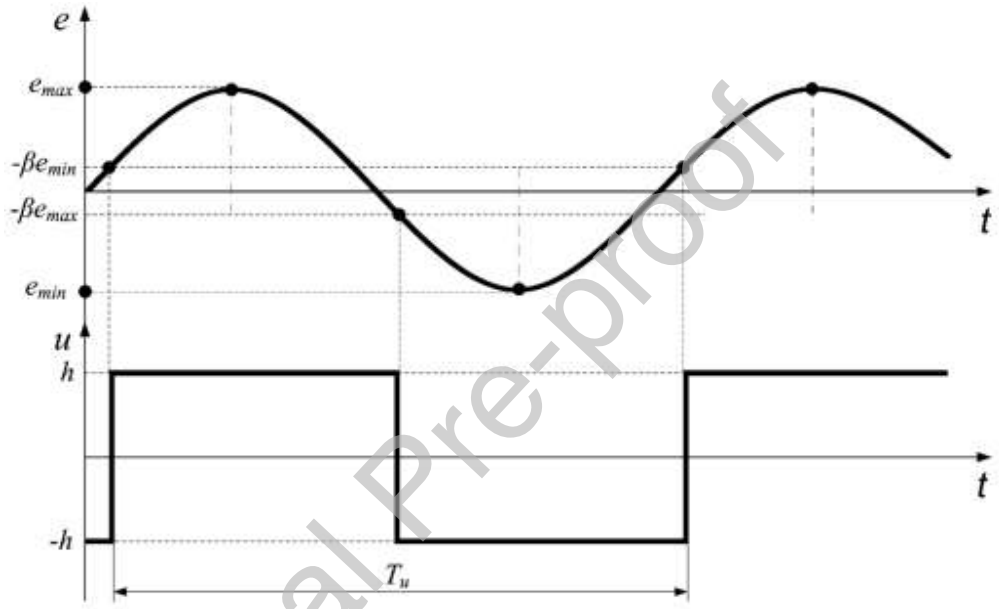

Figure 2 Typical input and output waveforms of the MRFT relay [16]

4. SHAPES ANALYSIS AND CATEGORIZATION

We use the generalized equations (8)-(11), and (13)-(16) to determine the time responses of each model (1)-(5). The responses are completely characterized by the situational parameters 'ζ and τ' and hence, the shapes are unique in distinct subsets of the entire domain of situational parameters. To probe further into these subsets, we first define a global domain of situational parameters as follows.

$$D_\tau := \{\tau_{\min} : \tau_{max} \in [0.05, 5]\}$$

$$D_\zeta := \{\zeta_{\min} : \zeta_{max} \in [0.1, 4]\} \quad (17)$$

The domain of the parameters has been selected in such a way as to cover realistic dynamics of many physical systems. The lower values of damping ratios, i.e. $\zeta = 0.1$, represent highly under-damped oscillatory response which a physical system rarely has. Similarly, a larger value of damping ratio, i.e. $\zeta = 4$, represents a highly over-damped response that can be modeled by either two 1st order systems (in a cascade connection). The domain of τ has been selected to represent dynamics normalized with respect to the dominant time constant $(\tau/T \to \tau)$. Hence, the models (1-5) are normalized compared to

actual physical systems dynamics. The delay of $\tau = 0.05$ indicates a very small ratio (meaning the delay is 20 times smaller than the time constant), and $\tau = 5$ indicates a very large delay (5 times larger than the time constant). The considered ranges cover many applications found in the industry [16].

After the selection of domains for each situational parameters, we simulate the MRFT cycles for all the parameters. We randomly pick numerous points within the domain for such purpose. It is observed that all MRFT cycles are exhibiting four unique shapes as presented in Figure 3.

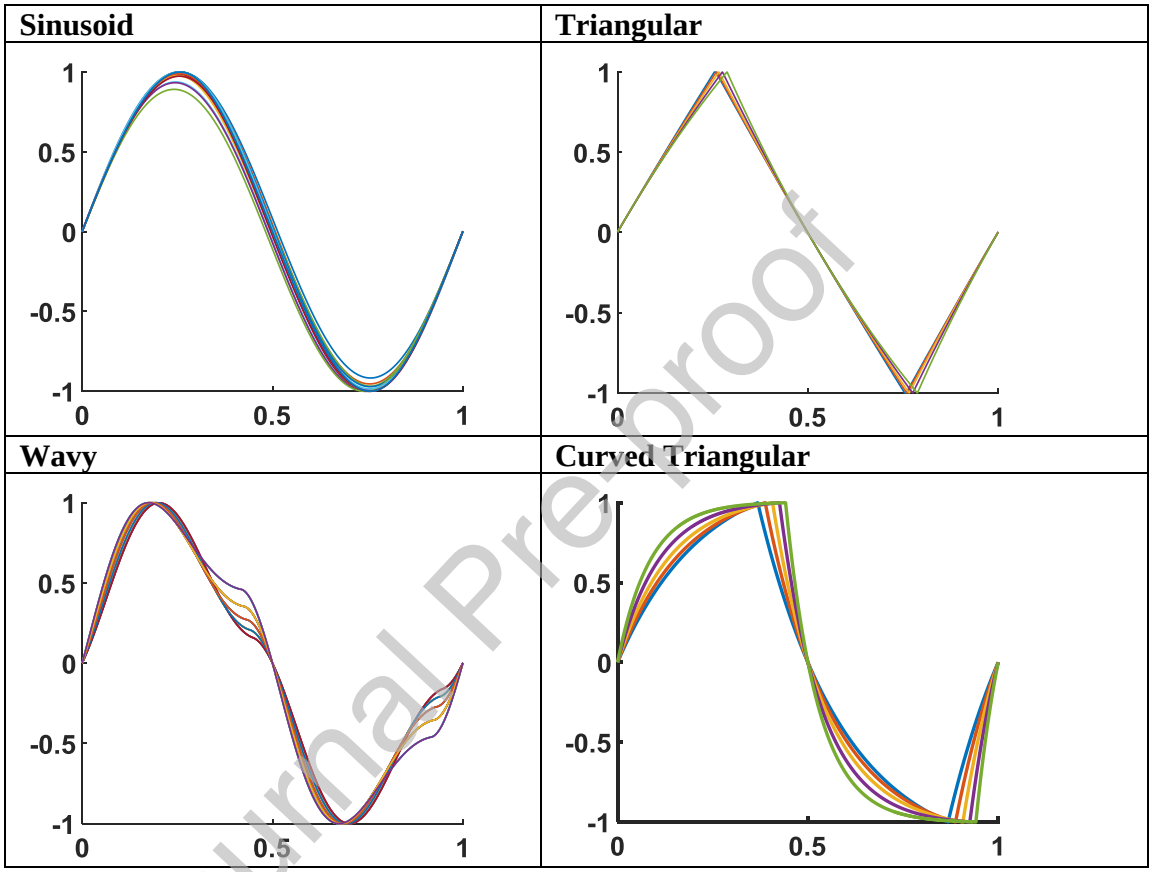

Figure 3 Four distinct shapes of one MRFT cycle of the five models

With the above four distinct shapes, we form a hierarchical categorization in two levels (Figure 4). The 1st level corresponds to the four distinct shapes while the second level corresponds to the five distinct models that exhibit these shapes. For the shape's categorization, only one cycle of the system's periodic response is sufficient to determine the form of shape. We may generate other classes as well provided they form different shapes in self-oscillatory mode however, to the author's knowledge, most physical system's response would closely match with one of the four shapes in Figure 3.

After the categorization of system models and shapes, the next important step is to divide the domain of all situational parameters into partitions. This is done to determine how the pattern of shapes are distributed across the entire domain of a model. Since a domain would exhibit numerous shapes, the partitioning must be done in such a way that each partition has a unique shape. We then develop tuning rules for each partition which are, in disguise, tuning rules for each shape. As, an example, Figure 5 shows how the response shapes of the second-order model are exhibited by an entire domain of

situational parameters. The response waveform can be categorized into three shapes: *triangular*, *wavy*, *and sinusoid*. It implies that the domain is to be divided into three partitions where the parameters in each partition would exhibit only one of the three shapes. Once we identify the shape partitions for all the model forms (1)-(5), we then compute the tuning rules for each shape.

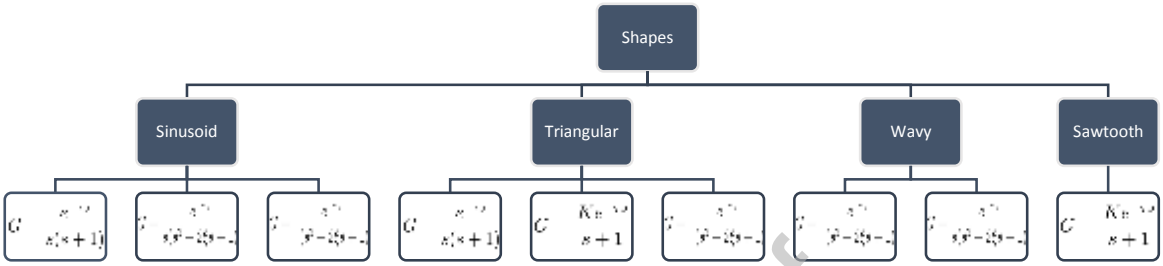

Figure 4 Hierarchical classification of shapes and system models (1)-(5)

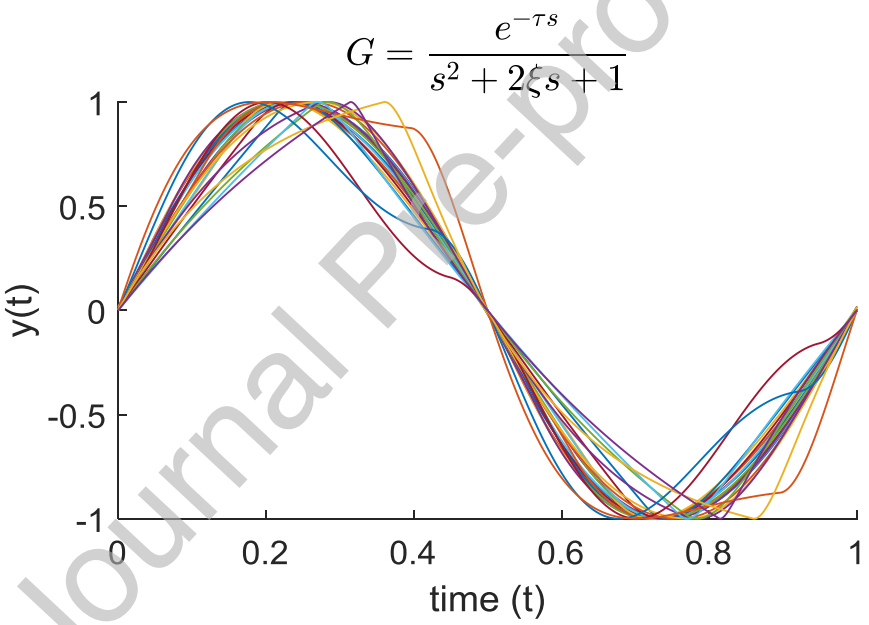

Figure 5 The MRFT cycles of various second-order models

Using this approach, we proceed with the categorization of shapes. We develop the equivalent state-space representation of all the models (1)-(5) and use the equations (8)-(11), and (13)-(16) in Matlab to generate time-domain responses of one MRFT cycle. A finite number of points (10 for each parameter) within the domain (17) is used to simulate the periodic responses. In the following subsections, we apply the above procedure on each model form (1)-(5) individually, and then later, we develop the tuning rules for each shape using the MRFT algorithm.

4.1. FIRST ORDER PLUS DEAD TIME MODEL:

The first-order model or commonly known as FOPDT model can be realized by the following matrices:

$$A = -1$$
$$B = 1 \qquad (18)$$
$$\mathrm{C} = 1$$

Using this state model with equations (8)-(11) we observe two shapes in the MRFT mode; triangular and curved triangular. The whole class of this model responses is dependent on one situational parameter "τ" whose domain is partitioned into two subsets corresponding to each shape. Figure 6 and Table 1 presents the shapes of all the response shapes and their distribution with respect to deadtime.

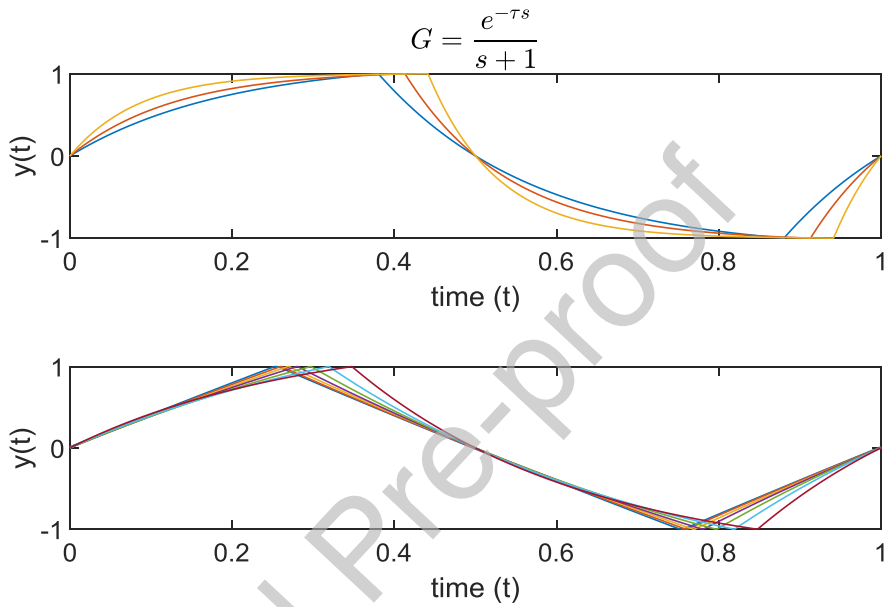

Figure 6 Two distinct Waveforms of MRFT cycle of 1st Order System

Table 1 Shapes distribution in 1st order model

τ	**1.50**	**1.71**	**1.96**	**2.24**	**2.56**	**2.93**	**3.35**	**3.83**	**4.37**	**5.00**
C_2	TRI	TRI	TRI	TRI	TRI	TRI	TRI	CT	CT	CT

4.2. INTEGRATOR WITH DEADTIME:

Various types of physical systems can be approximated by a simple integrator with deadtime. With regard to the shape, the integrator gives purely triangular waveform in the MRFT mode (Figure 7), where we use the following state-space model with equations (8)-(11) to generate the shapes:

$$A = 0$$
$$B = 1 \qquad (19)$$
$$\mathrm{C} = 1$$

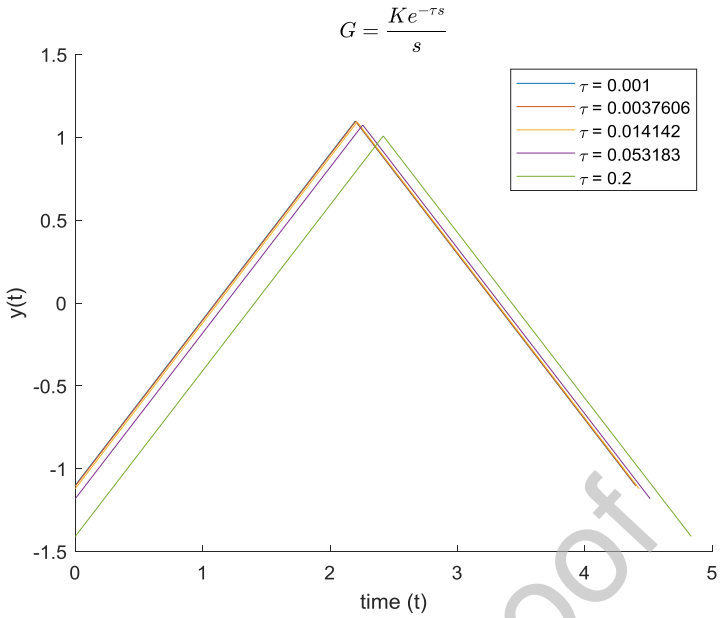

Figure 7 The MRFT cycle of Integrator

The shape is unique, and hence no variation is observed by using different values of deadtime for simple integrator model.

4.3. SECOND ORDER PLUS DEAD TIME MODEL:

For SOPDT models, we use the following canonical realization with the equations (8)-(11) to generate the shapes:

$$A = \begin{bmatrix} -2\zeta & -1 \\ 1 & 0 \end{bmatrix}$$
$$B = \begin{bmatrix} 1 \\ 0 \end{bmatrix} \quad (20)$$
$$C = [0 \quad 1]$$

The second-order model depicts three shapes in the MRFT mode: *sinusoidal*, *triangular*, *and wavy shape* (Figure 8). To visualize, how shapes are distributed w.r.t τ and ζ, we create a mesh of 10x10 parametric values and simulate the model in the MRFT setting at each value. Table 2 shows that there exists a continuum in the pattern of all shapes i.e. the shapes do not change abruptly while moving from one point to the other. Given the present domain, most portion of the shapes is dominated by a sinusoid. This is because second-order models are generally low pass in nature for a wide range of τ and ζ.

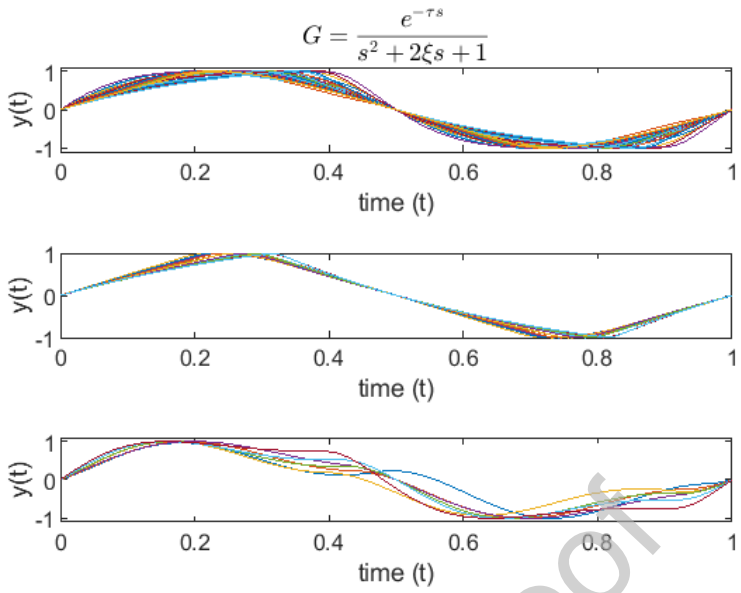

Figure 8 Three distinct shapes of the MRFT cycles of second-order models

Table 2 Distribution of shapes for 10x10 Second order models

ζ \ τ	**0.05**	**0.08**	**0.14**	**0.23**	**0.39**	**0.65**	**1.08**	**1.80**	**3.00**	**5.00**
0.10	SIN	SIN	SIN	SIN	SIN	SIN	SIN	SIN	SIN	WaVy
0.15	SIN	SIN	SIN	SIN	SIN	SIN	SIN	SIN	WaVy	WaVy
0.23	SIN	SIN	SIN	SIN	SIN	SIN	SIN	SIN	WaVy	WaVy
0.34	SIN	SIN	SIN	SIN	SIN	SIN	SIN	SIN	SIN	WaVy
0.52	SIN	SIN	SIN	SIN	SIN	SIN	SIN	SIN	SIN	WaVy
0.78	SIN	SIN	SIN	SIN	SIN	SIN	SIN	SIN	SIN	SIN
1.17	SIN	SIN	SIN	SIN	SIN	SIN	SIN	SIN	SIN	SIN
1.76	SIN	SIN	SIN	SIN	SIN	TRI	TRI	SIN	SIN	SIN
2.65	SIN	SIN	SIN	SIN	TRI	TRI	TRI	TRI	TRI	SIN
4.00	SIN	SIN	SIN	SIN	TRI	TRI	TRI	TRI	TRI	TRI

4.4. FIRST ORDER PLUS DEAD TIME MODEL WITH INTEGRATOR:

For this category of the model, we use the following state-space model with equations (13)-(16) to generate the shapes:

$$A = \begin{bmatrix} -1 & 0 \\ 1 & 0 \end{bmatrix}$$
$$B = \begin{bmatrix} 1 \\ 0 \end{bmatrix} \quad (21)$$
$$C = [0 \quad 1]$$

We observe two shapes for this model, sinusoid and triangular as shown in Figure 9. Table 3 shows how the shapes are distributed with respect to different values of deadtime.

$$= \frac{e^{-\tau s}}{s(s+1)}$$

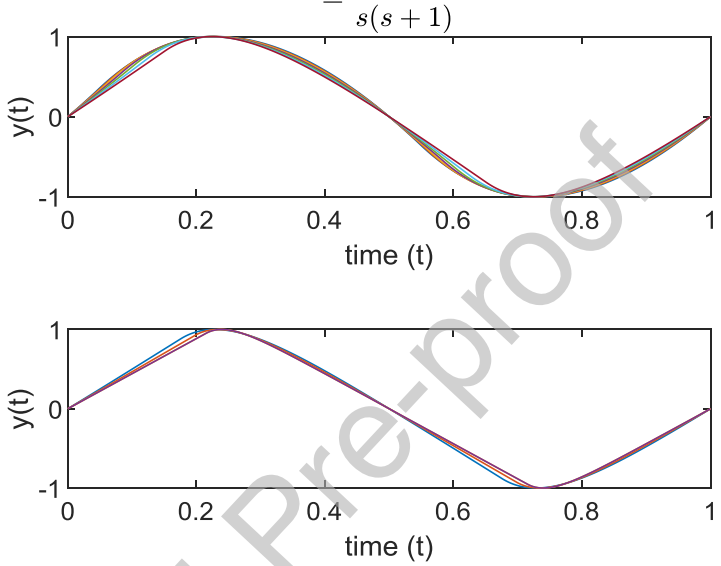

Figure 9 Two distinct shapes of the MRFT cycles of second-order models with integrator

Table 3 Distribution of shapes for1st order with integrator

τ	0.05	0.08	0.14	0.23	0.39	0.65	1.08	1.80	3.00	5.00
Shapes	"SIN"	"SIN"	"SIN"	"SIN"	"SIN"	"SIN"	"SIN"	"TRI"	"TRI"	"TRI"

4.5. SECOND ORDER PLUS DEAD TIME MODEL WITH INTEGRATOR:

For this category of the model, we use the following canonical form:

$$A = \begin{bmatrix} -2\zeta & -1 & 0 \\ 1 & 0 & 0 \\ 0 & 1 & 0 \end{bmatrix}$$
$$B = \begin{bmatrix} 1 \\ 0 \\ 0 \end{bmatrix} \quad (22)$$
$$\mathrm{C} = [0 \quad 0 \quad 1]$$

Using the above model with equations (13)-(16), and simulating them for different parameters give three distinct shapes (Figure 10). Table 4 shows how these shapes are distributed concerning different values of damping ratio and deadtime.

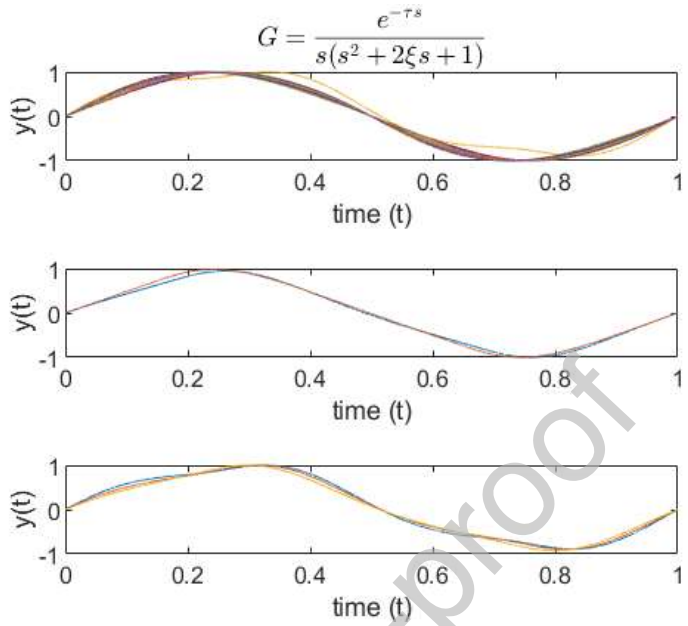

Figure 10 Three distinct MRFT cycles of Second Order With Integrator

Table 4 Partitioning of Domain for Second Order with Integrator

ζ \ τ	**0.05**	**0.08**	**0.14**	**0.23**	**0.39**	**0.65**	**1.08**	**1.80**	**3.00**	**5.00**
0.10	SIN	SIN	SIN	SIN	SIN	SIN	SIN	SIN	SIN	SIN
0.15	SIN	SIN	SIN	SIN	SIN	SIN	SIN	SIN	SIN	WaVy
0.23	SIN	SIN	SIN	SIN	SIN	SIN	SIN	SIN	SIN	WaVy
0.34	SIN	SIN	SIN	SIN	SIN	SIN	SIN	SIN	SIN	WaVy
0.52	SIN	SIN	SIN	SIN	SIN	SIN	SIN	SIN	SIN	TRI
0.78	SIN	SIN	SIN	SIN	SIN	SIN	SIN	SIN	SIN	TRI
1.17	SIN	SIN	SIN	SIN	SIN	SIN	SIN	SIN	SIN	SIN
1.76	SIN	SIN	SIN	SIN	SIN	SIN	SIN	SIN	SIN	SIN
2.65	SIN	SIN	SIN	SIN	SIN	SIN	SIN	SIN	SIN	SIN
4.00	SIN	SIN	SIN	SIN	SIN	SIN	SIN	SIN	SIN	SIN

5. PRINCIPLE OF DESIGNING OPTIMAL RULE FOR NON-PARAMETRIC TUNING, USING THE MRFT

After forming the classes for all the models, the next phase is to form tuning rules for these classes. We use the MRFT theory to formulate the rules. Using the MRFT test, the oscillations are generated in the third quadrant of a Nyquist plot. This is to ensure that the required gain margin is achieved once the PID with the dominant lag effect is connected with the system. We consider the PID of the following form:

$$G_c(s) = K_c(1 + \frac{1}{T_i s} + T_d s)$$

We denote the tuning rules as coefficients: c_1, c_2 and c_3 where the parameters of PID are directly related to these coefficients in the following form:

$$K_c = c_1 \frac{4h}{\pi a_0}, T_i = c_2 \frac{2\pi}{\Omega_0}, T_d = c_3 \frac{2\pi}{\Omega_0} \tag{23}$$

where a_0 and Ω_0 are the ultimate amplitude and frequency of the system under oscillation. To satisfy the gain margin specification, the tuning coefficients must satisfy the following:

$$\gamma_m c_1 \sqrt{1 + (2\pi c_3 - \frac{1}{2\pi c_2})^2} = 1 \tag{24}$$

$$\begin{aligned} \beta \quad &= -\sin \varphi_c(\Omega_0) = -\sin \arctan(2\pi c_3 - \frac{1}{2\pi c_2}) \\ &= -\frac{2\pi c_3 - \frac{1}{2\pi c_2}}{\sqrt{1 + (2\pi c_3 - \frac{1}{2\pi c_2})^2}} \end{aligned} \tag{25}$$

where "γ_m" is the required gain margin. The parameter 'β' determines the exact location of the solution of the harmonic balance equation in the Nyquist plot of the system.

For finding tuning coefficients in the above equation, we formulate the problem of Optimization Under Uncertainty (OUU) as proposed in [16], in which the cost function is parametrized. According to the OUU criterion, we first discretize the domain of situational parameters into a finite number of points. At each discrete point, an Integral Square Error (ISE) of the form $Q_{ISE} = \int_0^\infty e^2(t)\,\mathrm{d}t$ is minimized with respect to the tuning coefficients, where the error is produced in the reaction to the setpoint step input[2]. Such a procedure gives the optimal tuning coefficients at each point of situational parameters. Then we evaluate the maximum deterioration of each optimal rule over the entire domain of situational parameters. The tuning rule which shows the least deterioration is considered as the most optimal rule. This criterion is formulated as follows:

[2] Other integral performance criteria and reaction to a load step change were also used in [16]. In the present paper, we use only one criterion and only set point step, because the main emphasis is the partitioning of the models.

$$minimize\ \ g(c_1, c_2, c_3) = \max_{(\tau/T,\zeta)\in D}\{\frac{Q(c_1, c_2, c_3, \frac{\tau}{T}, \zeta)}{Q^*(\frac{\tau}{T}, \zeta)}\}$$
$$\text{subject to } \gamma_m c_1 \sqrt{1 + (2\pi c_3 - \frac{1}{2\pi c_2})^2} = 1 \tag{26}$$

In formulas (26), $Q^*(\frac{\tau}{T}, \zeta)$ is the solution of the minimization problem of $Q(c_1, c_2, c_3, \frac{\tau}{T}, \zeta)$ using the ISE cost, subject to constraints (24), for a given combination of $(\frac{\tau}{T}, \zeta)$. It should also be noted that with finding the optimal set of the tuning rule coefficients (c_1, c_2, c_3), we also find the optimal value of the parameter β of the MRFT through (25).

6. DEVELOPING TUNING RULES FOR THE SHAPES USING THE MRFT AND OPTIMIZATION UNDER UNCERTAINTY

The tuning rules are developed using the MRFT test and the OUU criterion of (26). Each system is first excited into a self-oscillatory mode with a gain margin of 2. Once the response achieves sustained oscillations, the ultimate frequency and the gain of the system are computed. The PID gains are then determined using equations (24)-(26) and the system with a tuned-PID is simulated for a step input for 20 seconds. The system's output is observed and ISE is recorded for the current values of tuning coefficients. This procedure is carried out for numerous values (ideally should be a 2x2 continuous mesh) of (c_2, c_3) until the least ISE is found. This problem is a convex optimization problem as the surface plot of ISE verses (c_2, c_3) comes out to be of paraboloid shape indicating that a global minimum ISE exists w.r.t (c_2, c_3). Therefore, we can use various search algorithms to find the global minimum, however, for this work we have used the built-in Matlab module of *"fminsearch"*. With this procedure, we obtain the most optimal (c_2, c_3) for one discrete point of the situational parameter (τ and/or ζ). Whereas, the situational parameters have an entire set of values corresponding to the particular shape and the system. So the same process of computing global ISE_{min} is repeated for all the discrete points of the situational parameter. This gives a set of minima corresponding to each point in the domain of situational parameters.

The next step is to evaluate the performance of each tuning rule across the entire domain using (26). This is done by computing the maximum deterioration of each coefficient w.r.t all the points representing a given shape. The optimal coefficients computed by the above procedure are tested here. We select each coefficient, turn by turn, and evaluate its ISE over the entire domain and then store only the maximum ISE. Once we have maximum ISEs (max-ISE) corresponding to all the coefficients pairs (c_2, c_3), we choose the pair with the least max-ISE. This ensures that the selected coefficient pair would cause the least deterioration with respect to a given shape and the form of system.

6.1. FIRST ORDER PLUS DEAD TIME MODEL:

Table 5 shows the tuning rules computed using the MRFT for all the points. The highlighted points show the most optimal coefficient computed using the OUU criterion for both sets. The tuning rules produced are for pure PI controller so $c_3 = 0$.

Table 5 Tuning rules (c_1,c_2) for first-order plus dead time model (Triangular in blue, Curved triangular in brown)

τ	**1.50**	**1.71**	**1.96**	**2.24**	**2.56**	**2.93**	**3.35**	**3.83**	**4.37**	**5.00**
C_1	0.50	0.50	0.50	0.50	0.49	0.48	0.46	0.45	0.45	0.45
C_2	6.05	3.78	2.33	1.40	0.87	0.56	0.40	0.33	0.32	0.33

6.2. INTEGRATOR WITH DEADTIME:

With the same procedure, the tuning coefficients of an integrator with deadtime are given in Table 6. It can be observed that tuning coefficients are invariant w.r.t delay 'τ' and hence one tuning rule $(c_1, c_2) = (0.5,0.48)$ suffices for all kinds of shape. For the integrator system, there is no need to apply the OUU criterion since we have only one optimal rule i.e. $(c_1, c_2, c_3) = (0.5,0.48,0)$.

Table 6 Tuning rules for the simple integrator

τ	**0.05**	**0.08**	**0.14**	**0.23**	**0.39**	**0.65**	**1.08**	**1.80**	**3.00**	**5.00**
C_1	0.48	0.48	0.48	0.48	0.48	0.48	0.48	0.48	0.48	0.48
C_2	0.50	0.50	0.50	0.50	0.50	0.50	0.50	0.50	0.50	0.50
C_3	0	0	0	0	0	0	0	0	0	0

6.3. SECOND ORDER PLUS DEAD TIME MODEL:

For this category of the model, we derive the tuning rules for three shapes. Table 7-Table 8 shows optimal rules computed independently for each shape partition, where the highlighted values show the most optimal tuning rules computed through the OUU criterion for each partition. The tuning rules produced are for pure PI controller so $c_3 = 0$.

Table 7 Tuning rules (c_1) for Second Order Model (Sinusoid in red, Triangular in blue, Wavy in black)

ζ \ **τ**	**0.05**	**0.08**	**0.14**	**0.23**	**0.39**	**0.65**	**1.08**	**1.80**	**3.00**	**5.00**
0.10	0.49	0.49	0.48	0.39	0.06	0.06	0.08	0.20	0.26	0.39
0.15	0.48	0.49	0.48	0.44	0.12	0.07	0.12	0.20	0.26	0.37
0.23	0.50	0.47	0.48	0.46	0.39	0.19	0.17	0.20	0.29	0.35
0.34	0.50	0.50	0.49	0.47	0.45	0.35	0.29	0.30	0.34	0.38
0.52	0.50	0.50	0.50	0.49	0.47	0.44	0.39	0.39	0.40	0.41
0.78	0.50	0.50	0.50	0.50	0.49	0.48	0.45	0.43	0.44	0.44

1.17	0.50	0.50	0.50	0.50	0.50	0.49	0.48	0.47	0.45	0.45
1.76	0.50	0.50	0.50	0.50	0.50	0.50	0.49	0.48	0.47	0.46
2.65	0.50	0.50	0.50	0.50	0.50	0.50	0.50	0.49	0.48	0.49
4.00	0.50	0.50	0.50	0.50	0.50	0.50	0.50	0.50	0.49	0.00

Table 8 Tuning rules (c_2) for Second Order Model (Sinusoid in red, Triangular in blue, Wavy in black)

ζ τ	**0.05**	**0.08**	**0.14**	**0.23**	**0.39**	**0.65**	**1.08**	**1.80**	**3.00**	**5.00**
0.10	0.95	0.91	0.51	0.20	0.02	0.02	0.03	0.07	0.10	0.20
0.15	0.56	0.65	0.54	0.28	0.04	0.02	0.04	0.07	0.10	0.17
0.23	3.32	0.44	0.54	0.36	0.20	0.07	0.06	0.07	0.12	0.16
0.34	5.82	2.36	0.69	0.47	0.31	0.15	0.11	0.12	0.15	0.18
0.52	8.85	3.88	1.67	0.81	0.48	0.30	0.20	0.19	0.21	0.23
0.78	9.12	5.52	2.88	1.45	0.81	0.52	0.35	0.28	0.28	0.31
1.17	9.22	8.42	4.34	2.38	1.38	0.85	0.57	0.41	0.33	0.34
1.76	9.62	8.94	6.23	3.82	2.25	1.41	0.93	0.62	0.44	0.39
2.65	51.05	20.43	9.88	6.04	3.62	2.30	1.48	0.95	0.63	0.53
4.00	73.72	30.43	14.70	9.48	6.27	3.66	2.30	1.45	0.95	0.80

6.4. FIRST ORDER PLUS DEAD TIME MODEL WITH INTEGRATOR:

The same strategy of the first-order system is used for this model. However, we incorporate an additional derivative gain this time. This is because of the presence of integrator, the tuning rules based on PI alone are insufficient to produce a satisfactory control. Table 9 shows the tuning rules for the given range of 'τ'. Also, are highlighted the most optimal tuning rules based on the OUU criterion for each shape.

Table 9 Tuning rules for1st order with integrator (Sinusoid in red, Triangular in blue)

τ	**0.05**	**0.08**	**0.14**	**0.23**	**0.39**	**0.65**	**1.08**	**1.80**	**3.00**	**5.00**
C_1	0.21	0.19	0.19	0.18	0.20	0.24	0.27	0.32	0.35	0.38
C_2	84512	83804	9140	183	1304	127	99	486	66.9	52.
C_3	0.35	0.39	0.38	0.42	0.36	0.3	0.24	0.196	0.164	0.134

6.5. SECOND ORDER PLUS DEAD TIME MODEL WITH INTEGRATOR:

We compute the tuning coefficients for this case in the same way as we did for the second-order model. Also, because of the presence of an integrator, we incorporate the derivative part to constitute a full PID controller. As in the second-order model, three shapes are observed, so we divide the domain of the situational parameter into three partitions. Then we compute the tuning coefficients (c_1,c_2,c_3) for each shape/partition. Table 10-Table 12 shows these coefficients computed using the optimization procedure. Also, are highlighted the most optimal coefficients using the OUU criterion.

Table 10 Tuning coefficient c_1 for all shapes (Sinusoid in red, Triangular in blue, Wavy in black)

ζ^{τ}	**0.05**	**0.08**	**0.14**	**0.23**	**0.39**	**0.65**	**1.08**	**1.80**	**3.00**	**5.00**
0.10	0.25	0.39	0.50	0.29	0.27	0.34	0.41	0.48	0.49	0.44
0.15	0.22	0.30	0.43	0.49	0.41	0.41	0.45	0.50	0.48	0.45
0.23	0.18	0.27	0.34	0.45	0.50	0.49	0.49	0.50	0.47	0.45
0.34	0.15	0.20	0.27	0.36	0.43	0.48	0.49	0.48	0.45	0.44
0.52	0.13	0.16	0.19	0.25	0.32	0.37	0.42	0.43	0.42	0.43
0.78	0.12	0.14	0.17	0.20	0.24	0.28	0.32	0.35	0.37	0.41
1.17	0.12	0.14	0.15	0.17	0.19	0.22	0.25	0.29	0.33	0.39
1.76	0.13	0.13	0.14	0.16	0.17	0.19	0.21	0.24	0.27	0.36
2.65	0.14	0.12	0.14	0.15	0.16	0.17	0.18	0.20	0.24	0.34
4.00	0.50	0.50	0.11	0.50	0.15	0.50	0.16	0.50	0.21	0.31

Table 11 Tuning coefficient c_2 for all shapes (Sinusoid in red, Triangular in blue, Wavy in black)

ζ^{τ}	**0.05**	**0.08**	**0.14**	**0.23**	**0.39**	**0.65**	**1.08**	**1.80**	**3.00**	**5.00**
0.10	2.01	1.83	1.73	1.69	2.04	2.96	5.98	26	313	28
0.15	3.81	3.36	3.08	2.97	3.12	11.5	8.88	28	441	40
0.23	100	59	6.11	5.41	5.47	6.20	9.85	35	210	357
0.34	117	152	100	55	12	12	16	36	488	811
0.52	24	52	158	115	80	52	38	39	38	51
0.78	275	202	55	151	125	78	80	64	53	41
1.17	73	136	218	120	158	136	119	92	197	249
1.76	259	252	156	211	527	160	148	127	43	106
2.65	236	186	209	227	213	254	182	276	111	12

4.00	314	1131	506	1591	229	1775	218	1359	570	2.46

Table 12 Tuning coefficient c_3 for all shapes (Sinusoid in red, Triangular in blue, Wavy in black)

ζ τ	**0.05**	**0.08**	**0.14**	**0.23**	**0.39**	**0.65**	**1.08**	**1.80**	**3.00**	**5.00**
0.10	0.29	0.14	0.03	0	0	0	0	0	0.04	0.08
0.15	0.34	0.22	0.10	0	0	0	0	0	0.05	0.076
0.23	0.40	0.24	0.18	0.08	0.00	0	0	0.01	0.06	0.074
0.34	0.52	0.37	0.24	0.15	0.09	0.05	0.04	0.05	0.07	0.08
0.52	0.60	0.48	0.38	0.27	0.19	0.14	0.11	0.10	0.10	0.098
0.78	0.63	0.54	0.45	0.37	0.30	0.24	0.19	0.16	0.14	0.11
1.17	0.64	0.57	0.49	0.44	0.38	0.32	0.27	0.23	0.18	0.13
1.76	0.59	0.57	0.53	0.48	0.45	0.39	0.35	0.30	0.25	0.15
2.65	0.53	0.62	0.55	0.52	0.49	0.45	0.41	0.36	0.30	0.17
4.00	0.02	0.01	0.74	0.01	0.52	0.01	0.46	0	0.35	0.21

6.6. SHAPE-SPECIFIC TUNING RULES:

So far, we have developed the tuning rules for all the shapes produced by each model (1)-(5). As a final step, we merge the tuning rules that correspond to identical shapes and identical type of the models. This is necessary because the models remain unknown; the only information that is assume to be known is whether the process is self-regulating or integrating. At the same time, the information that becomes available after conducting the test is the shape that can be used for a more accurate tuning. Based on Figure 4, we determine that all the cases are distinct with the exception of two shapes. The first is the sinusoid shape of the integrating FOPDT and SOPDT models and second is the triangular shape of the non-integrating FOPDT and SOPDT models.

Hence, we combine the tuning rules for these similar cases on the following basis:

1. For the sinusoid shapes of the integrating FOPDT and SOPDT models, we have the rules as $(c_1, c_2, c_3) = (0.19,9140,0.38)$, and $(0.18,182,0.41)$ respectively. The rules are similar, as the high value of coefficient c_2 would make the integrator almost zero. The overall running rule for the sinusoid shape can be produced through the second stage of the OOU (26).

2. For the triangular shapes of non-integrating FOPDT and SOPDT models, we have different tuning rules which are $(c_1, c_2, c_3) = (0.49,0.87,0)$, and $(0.5,1.48,0)$ respectively. So for these cases, we combine the tuning rules using the OUU principle again by determining the deterioration of one rule over the other.

   The deteriorations of each rule are found using the criterion (26) as follows:

- The FOPDT Triangular optimal tuning rule applied to SOPDT triangular optimum point gives the deterioration as 1.0365.
- The SOPDT Triangular optimal tuning rule applied to FOPDT triangular optimum point gives the deterioration as 1.0475.

The above implies the FOPDT Triangular optimal tuning rule is causing lesser deterioration hence it is more optimal. Similarly, for the sinusoid shapes of the integrating FOPDT and SOPDT models, it is found that the tuning rule of the integrating SOPDT which is $(c_1, c_2, c_3) = (0.18,182,0.41)$ causes lesser deterioration and hence is more optimal.

Finally we tabulate all the tuning rules in the Table 13.

Table 13 Tuning rules based on the classification of the shapes

Shape	System type	TUNING RULE (c_1, c_2 and c_3)
Sinusoid	Non-integrating	(0.5,1.67,0)
	Integrating	(0.18,182,0.41)
Triangular	Non-integrating	(0.49,0.87,0)
	Integrating	(0.35,66.9,0.164)
Curved Triangular	Non-integrating	(0.45,0.32,0)
	Integrating	N/A *
Wavy	Non-integrating	(0.35,0.16,0)
	Integrating	(0.45,357,0.074)

*Not applicable

7. CLASSIFICATION OF A GIVEN RESPONSE FOR CONTROL TUNING

Let us now discuss how we can apply the above tuning rules on a given system. First, we need to have *a priori* knowledge of some characteristics of the system's dynamic model, in particular, integrating or self-regulating. This knowledge is essential to determine the correspondence between the given system and the above LTI models. Such knowledge is usually available. For example, it is known that the gas a liquid flow process is self-regulating, liquid level in a tank integrating, etc. Once, the class of the model is determined, we then carry out a self-oscillatory test of the system to examine the shape of its output response. The response is likely not to coincide exactly with one of the shapes of our classes. In such a case, we have to perform classification of the response using a certain mathematical tool that determines its resemblance with one of the class-shapes. Once the class is determined, the tuning rule of that class becomes applicable to that system.

To classify a given system's response, a classification algorithm is required to be implemented to quantify the maximum similarity between the given response and the class response. Among many approaches, one way of implementing the classification is to use the cross-correlation metric as follows:

$$r_{xy}(\tau) = \frac{\sum_t (x(t) - \overline{x})(\mathrm{y}(t,\tau) - \overline{y})}{\sqrt{\sum_t (\mathrm{x}(t) - \overline{x})^2 \sum (\mathrm{y}(t,\tau) - \overline{y})^2}} \tag{27}$$

To implement the function (27), the given dataset of the signal is transformed into a scale comparable with our class response. For this, normalization is carried out in which the amplitude and time axis of the signal dataset is scaled to unity. Also, the relation (27) gives a correlation as a function of the temporal difference between the two signals. However, the function attains a maximum value when the phase difference between the signals is zero. We need only to account for this maximum correlation. This procedure is applied for a given signal against all the predefined class signals. The class which gives the maximum correlation will indicate the maximum similarity with the corresponding signal and hence the tuning rule of that class becomes applicable to the system.

8. EXAMPLE

We use a case of a FOPDT system to demonstrate the tuning procedure. Consider the FOPDT system as follows:

$$W_p(s) = \mathrm{e}^{-\mathrm{s}} \frac{1}{\mathrm{s} + 1}$$

It is also assumed that the output is corrupted with the noise of SNR=4. The tuning procedure is carried out in four steps as follows:

Step 1-*Excite the MRFT oscillations*: As a first step, the system is excited into MRFT mode while using a nominal value of 'β'. Figure 11 illustrates the output of the MRFT waveform for $\beta = 0$. Only one cycle is extracted from the waveform whose dataset is also normalized for the subsequent classification.

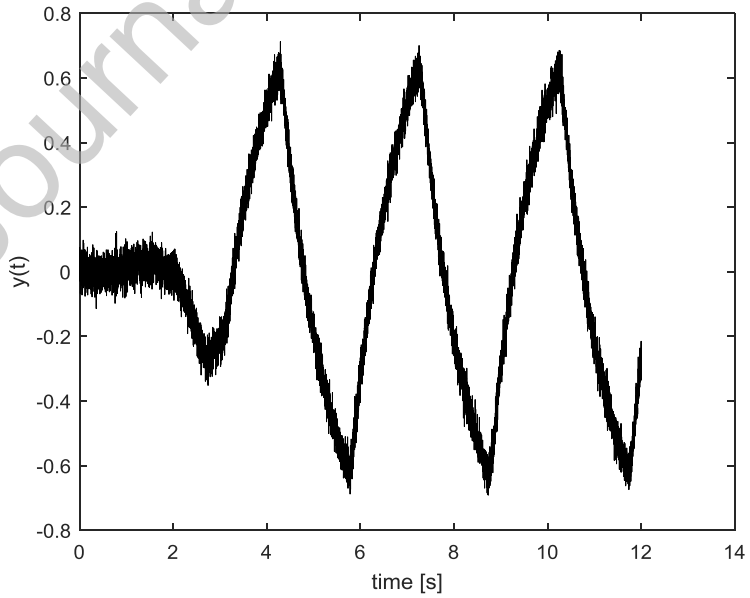

Figure 11 The MRFT cycle of the system

Step 2*- Determine the class of Shape and the tuning rule:* For the classification, we rely on the *apriori* knowledge that the form of the system fits with a 1st order system, hence we classify the response into the shapes of first-order classes. The class signals are picked such that they correspond to the models with the most optimal tuning rule that causes the least deterioration in their respective domains. However, this condition may be relaxed for 2nd order responses, as it is observed that, after normalization, the majority of sinusoidal shapes get squeezed into the same sinusoidal shape with unity amplitude and time. The classification is carried out using the cross-correlation function (27).

After performing the correlation using (27), we acquire the following maximum correlation values (see Table 14):

Table 14 Correlation of the given response with class responses

Correlation	Curved Tri-angular	Triangular
$r_{xy}(\tau)$	0.98	0.97

So, the maximum correlation comes out to be for the Curved Triangular shape, which is accurate since the sample response is the output of the 1st order system with a curved triangular shape. Hence, the tuning rule of the FOPDT Curved Triangular shape, which is ($c_1 = 0.45, c_2 = 0.32,$), is applicable to this example system.

Step 3*- Determine ultimate parameters from the MRFT oscillations:* The system, hence, is re-simulated in MRFT mode using the given tuning coefficients (Figure 12). From the oscillations in Figure 11, we compute the ultimate frequency and ultimate amplitude as $\Omega_0 = 1.59$ and $a_0 = 0.7557$ respectively.

Step 4*- Compute the PID gains:* Using the equation (23), the PID gains are computed as:

$$K_c = 0.75, T_i = 0.59, T_d = 0$$

Figure 13 shows the simulation response with the setpoint of 1. Evidently, the output is regulated at the given setpoint with very low overshoot and settling time.

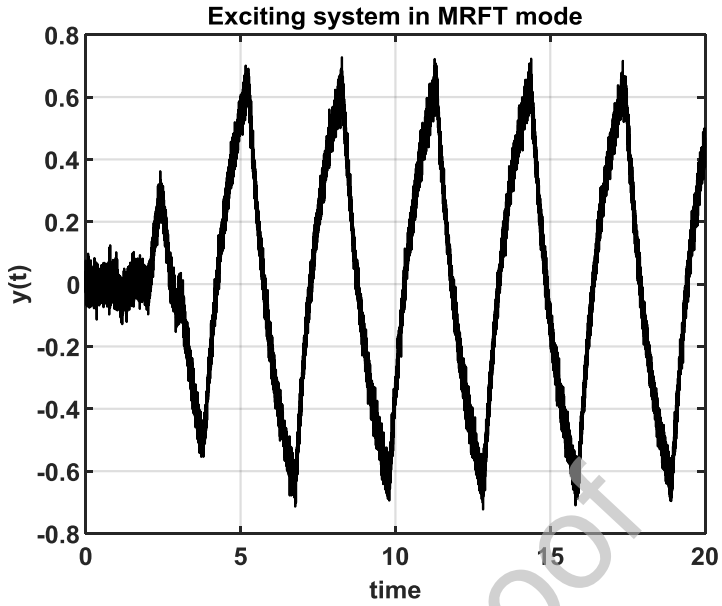

Figure 12 The MRFT oscillations using the tuning coefficients

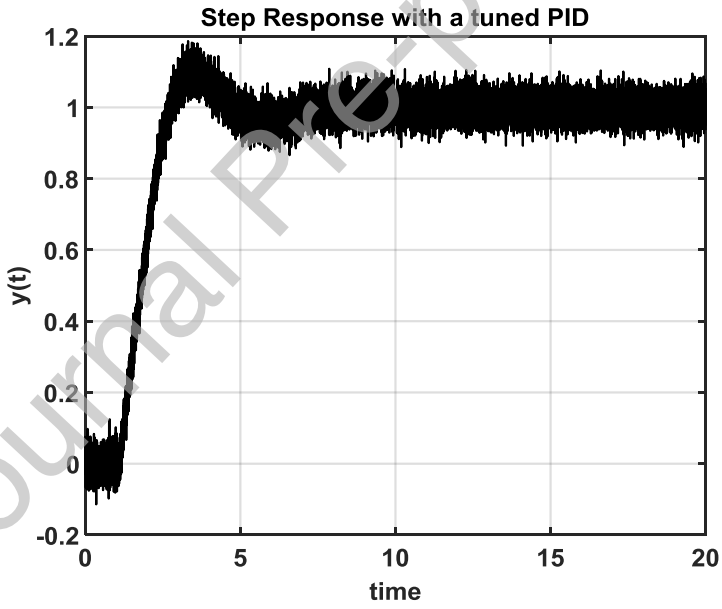

Figure 13 Step response using the tuning rule of the response Class

Other's classification techniques can also be explored as a further extension of this work that, for example, can transform the response data into a 2D dataset and use the Deep Learning-based classification approaches.

9. CONCLUSION

In this work, PID tuning has been investigated using the characteristics of the shape of the self-oscillatory response and the form of the system's model. In this respect, we have used the MRFT and Optimum Non-parametric Tuning method to develop tuning rules for several classes, where each class represents a unique combination of the system's model and the oscillatory shape. For the application of

the tuning rules, the response of the system is first classified into one of the classes based on maximum resemblance with the class response. For this, different classification algorithms can be applied however we have used the mathematical tool of cross-correlation. After, classification, the tuning rule for the class is applied to that system. The proposed approach is illustrated by an example.

10. ACKNOWLEDGMENTS

The authors acknowledge the support provided by the Khalifa University of Science and Technology Award No. RC1-2018-KUCARS, Project CIRA-2020-082 and Project EX2019-011.

11. REFERENCES

[1] J. G. Ziegler and N. B. Nichols, "Optimum settings for automatic controllers," *trans. ASME*, vol. 64, no. 11, 1942.

[2] G. H. Cohen and G. A. Coon, "Theoretical consideration of retarded control," *Trans. Asme*, vol. 75, pp. 827–834, 1953.

[3] K. J. Åström and T. Hägglund, "Automatic tuning of simple regulators with specifications on phase and amplitude margins," *Automatica*, vol. 20, no. 5, pp. 645–651, 1984.

[4] K. J. Åström and T. Hägglund, *PID controllers: theory, design, and tuning*, vol. 2. Instrument society of America Research Triangle Park, NC, 1995.

[5] T. K. Kiong, W. Qing-Guo, H. C. Chieh, and T. J. Hägglund, *Advances in PID control*. Springer, 1999.

[6] K. K. Tan, T. H. Lee, and Q. G. Wang, "Enhanced automatic tuning procedure for process control of PI/PID controllers," *AIChE J.*, vol. 42, no. 9, pp. 2555–2562, 1996.

[7] M. Friman and K. V Waller, "A two-channel relay for autotuning," *Ind. Eng. Chem. Res.*, vol. 36, no. 7, pp. 2662–2671, 1997.

[8] M. I. Castellanos, I. Boiko, and L. Fridman, "Parameter identification via modified twisting algorithm," *Int. J. Control*, vol. 81, no. 5, pp. 788–796, 2008.

[9] C.-C. Yu, *Autotuning of PID controllers: A relay feedback approach*. Springer Science & Business Media, 2006.

[10] I. M. Boiko, "Loop tuning with specification on gain and phase margins via modified second-order sliding mode control algorithm," *Int. J. Syst. Sci.*, vol. 43, no. 1, pp. 97–104, 2012.

[11] M. Haekal and I. Boiko, "MRFT based identification of process dynamics," in *2014 13th International Workshop on Variable Structure Systems (VSS)*, 2014, pp. 1–2.

[12] I. Matraji, W. Wang, I. Boiko, A. Al-Durra, and I. Y. Abushawish, "Simulator and Controller Tuning/Testing Rig for Artificial Gas Lift," in *Abu Dhabi International Petroleum Exhibition & Conference*, 2017.

[13] M. S. Chehadeh and I. Boiko, "Design of rules for in-flight non-parametric tuning of PID controllers for unmanned aerial vehicles," *J. Franklin Inst.*, vol. 356, no. 1, pp. 474–491, 2019.

[14] H. Al Shehhi and I. Boiko, "MRFT-based design of robust and adaptive controllers for gas loop of oil–gas separator," *Cogent Eng.*, vol. 2, no. 1, p. 999415, 2015.

[15] H. Hussein, A. Al-Durra, and I. Boiko, "Design of gain scheduling control strategy for artificial gas lift in oil production through modified relay feedback test," *J. Franklin Inst.*, vol. 352, no. 11, pp. 5122–5144, 2015.

[16] I. Boiko, "Non-parametric tuning of PID controllers," in *Advances in Industrial Control*, no. 9781447144649, 2013, pp. 9–23.

[17] I. Boiko, "Design of non-parametric process-specific optimal tuning rules for PID control of flow

loops," *J. Franklin Inst.*, vol. 351, no. 2, pp. 964–985, 2014.
[18] W. L. Luyben, "Getting more information from relay-feedback tests," *Ind. Eng. Chem. Res.*, vol. 40, no. 20, pp. 4391–4402, 2001.
[19] T. Thyagarajan and C.-C. Yu, "Improved autotuning using the shape factor from relay feedback," *Ind. Eng. Chem. Res.*, vol. 42, no. 20, pp. 4425–4440, 2003.
[20] T. Thyagarajan, C.-C. Yu, and H.-P. Huang, "Assessment of controller performance: a relay feedback approach," *Chem. Eng. Sci.*, vol. 58, no. 2, pp. 497–512, 2003.
[21] R. C. Panda and C.-C. Yu, "Shape factor of relay response curves and its use in autotuning," *J. Process Control*, vol. 15, no. 8, pp. 893–906, 2005.
[22] C. Esakkiappan and T. Thyagarajan, "Identification of inverse response process with time delay using relay feedback test," *Int. J. Comput. Appl. Technol.*, vol. 44, no. 4, pp. 269–275, 2012.
[23] T. Thyagarajan, C. Esakkiappan, and V. Sujatha, "Modeling and control of Inverse Response process with time delay using relay feedback test," in *Proceedings of the 2010 International Conference on Modelling, Identification and Control*, 2010, pp. 494–499.
[24] T. Liu, F. Gao, and Y. Wang, "A systematic approach for on- line identification of second- order process model from relay feedback test," *AIChE J.*, vol. 54, no. 6, pp. 1560–1578, 2008.
[25] S. Nikita and M. Chidambaram, "Improved relay auto-tuning of PID controllers for unstable SOPTD systems," *Chem. Eng. Commun.*, vol. 203, no. 6, pp. 769–782, 2016.
[26] Z. Ya, "Tsypkin, Relay Control Systems." Cambridge University Press, 1984.
[27] I. Boiko, *Discontinuous control systems: frequency-domain analysis and design*. Springer Science & Business Media, 2008.
[28] B. Hamel, "Contribution a l'etude mathematique des systemes de reglage par tout-ou-rien," *CEMV Serv. Tech. Aeronaut.*, vol. 17, p. 1949, 1949.
[29] I. Boiko, "Oscillations and Transfer Properties of Relay Servo Systems With Integrating Plants," *IEEE Trans. Automat. Contr.*, vol. 53, no. 11, pp. 2686–2689, 2008.
[30] R. Fitts, "two counterexamples to Aizerman's conjecture", IEEE Trans. On Automatic Control, Vol. 11, No. 3, pp. 553 – 556, 1966.
[31] Visioli, A., 2012. Research trends for PID controllers. Acta Polytechnica, 52(5).

Declaration of interests

The authors declare that they have no known competing financial interests or personal relationships that could have appeared to influence the work reported in this paper.